In presenting the dissertation as a partial fulfillment of the requirements for an advanced degree from the Georgia Institute of Technology, I agree that the Library of the Institute shall make it available for inspection and circulation in accordance with its regulations governing materials of this type. I agree that permission to copy from, or to publish from, this dissertation may be granted by the professor under whose direction it was written, or, in his absence, by the Dean of the Graduate Division when such copying or publication is solely for scholarly purposes and does not involve potential financial gain. It is understood that any copying from, or publication of, this dissertation which involves potential financial gain will not be allowed without written permission.

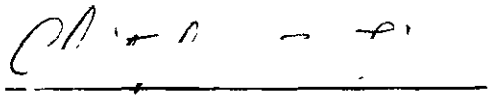

7/25/68

CONFORMATIONAL ANALYSIS OF INSULIN IN VARIOUS STATES BY RAMAN SPECTROSCOPY

A THESIS

Presented to

the Faculty of the Division of Graduate

Studies and Research

by

Christopher Soundang Liu

In Partial Fulfillment

of the Requirements for the Degree

Master of Science in Chemistry

Georgia Institute of Technology

July, 1972

CONFORMATIONAL ANALYSIS OF INSULIN IN VARIOUS

STATES BY RAMAN SPECTROSCOPY

Approved:

Nai-Teng Yu, Chairman

R. H. Felton

J. C. Powers

Date approved by Chairman:

ACKNOWLEDGMENTS

It is my pleasure to acknowledge with very sincere thanks the patient guidance and encouragement of Dr. Nai-Teng Yu during the course of this work.

I am indebted also to Dr. Donald C. O'Shea for granting me the use of his Raman Spectrometer and his many assistances in instrument operation.

Consistent encouragement from my parents, uncle, and aunt will never be forgotten.

Special thanks are due to my wife, Lily, for patience and encouragement during the course of this work, and for typing several drafts of this thesis.

TABLE OF CONTENTS

LIST OF TABLES

LIST OF ILLUSTRATIONS

SUMMARY

Glucagon, a polypeptide hormone of 29 amino acid residues, was used as a model compound to study the Raman spectral changes associated with the α-helix-to-coil and coil-to-β transitions in proteins. The amide III frequency of crystalline glucagon at 1266 cm^{-1} has shifted to 1248 cm^{-1} upon dissolution in acidic aqueous solution (pH 2.25) and then to 1232 cm^{-1} on gel formation at 26°C. These frequencies are very similar to those of α-helical poly-L-alanine, random-coiled poly-L-glutamic acid and antiparallel-β poly-glycine I, respectively. Although the amide I line of the random-coiled glucagon in dilute aqueous solution was not observed because of the masking of the 1640 cm^{-1} line due to water, the characteristic amide I frequencies of α-helical and β-glucagon were observed at 1658 and 1672 cm^{-1}, respectively. The latter has shown up in the spectrum as a very intense sharp line (half-width approximately 15 cm^{-1}) on the sloping background of water.

On the basis of the spectroscopic data obtained from glucagon, the author has carried out a detailed study on Raman spectra of native and denatured insulin in the solid state and aqueous solution. The spectra reported in this thesis have been obtained with the excitation of the 514.5 nm radiation from an argon-ion laser. For the first time, striking Raman spectral changes on denaturation of proteins were observed. Comparison between the native and denatured spectra indicates that extensive conformational changes have taken place in the conversion of native

to denatured fibrous insulin and that fibrous insulin exists predominantly in a β-conformation as proposed by Ambrose and Elliott in 1951. This finding is significant because in the past the conformation of fibrous insulin had been considered as the linear aggregate of slightly distorted globular insulin (Waugh, 1944; Koltun et al., 1954; Reithel, 1963; Beaven et al., 1961).

In addition, a Raman spectrum of proinsulin in the solid state was obtained and compared to that of insulin. A total of 11 lines, known to be conformation-dependent, was found to agree between the two spectra. This suggests that the insulin moiety of proinsulin exists in a conformation nearly the same as insulin, consistent with the conclusions of Frank and Veros (1968).

CHAPTER I

INTRODUCTION

Raman spectroscopy is based on an analysis of the radiation scattered from the surface of material or by passing the incident beam through a transparent liquid. It provides the same kind of information as infrared, namely the characteristic frequencies and intensities of molecular vibrations and rotations.

A change in the polarizability or induced dipole moment of the molecule during the molecular vibration will result in a vibrational mode in the Raman scattering of photons whereas changing the dipole moment of the bond will lead to the infrared absorption. Thus polar groups, which have large dipole moments, strongly absorb infrared radiation whereas the readily polarized nonpolar groups give rise to strong Raman scattering. In addition, symmetrical modes are generally strong Raman scatterers whereas antisymmetrical modes are more prominent in infrared spectra. In general, the more symmetrical a molecule the greater the differences between the Raman and infrared spectra. Since Raman spectroscopy and infrared have different physical bases, they provide complementary molecular data. Although the comparison between the two spectra will often aid in the assignments of the frequencies of the various vibrational modes, sometimes one can be used while the other cannot.

There are several advantages which make the Raman effect superior

to infrared absorption in the study of biological materials. The first of these is its relatively weak scattering of water, which gives rise to only one moderately intense band in the region 3200 to 3600 cm^{-1} and the relatively weak bands near 1640, 800, 450, and 175 cm^{-1}. Thus it becomes possible to use Raman technique to study the structural difference between the crystalline and aqueous proteins. The other advantage is the small sample size because of the availability of the high power laser beam as excitation source.

The potentiality of Raman spectroscopy for the study of proteins was first appreciated by Edsall. As early as 1938, he made a Raman study of egg albumin with practically no results (Edsall, 1938). In 1958, Edsall and Garfinkel reported the first Raman spectrum of a naturally occurring protein, lysozyme, in which a total of 14 faint lines was observed. After the advent of the laser, Tobin (1968) obtained the laser Raman spectra of crystalline lysozyme, pepsin, and chymotrypsin but the poor signal-to-noise ratio of the spectra prevented him from obtaining structural information. In 1970, Lord and Yu made the first detailed interpretation of the laser Raman spectra of lysozyme, ribonuclease, and α-chymotrypsin in aqueous solution. The spectra were obtained with He-Ne laser excitation (about 30 mw at 632.8 nm). Their major results may be summarized:

(1) Raman spectroscopy is useful in providing direct evidence concerning the presence and number of disulfide cross-links in proteins, and may also be useful in studying the local geometry of the C-S-S-C links.

(2) The aromatic side groups give rise to intense and sharp lines. The frequencies of these lines are not sensitive to changes in conformation or state of aggregation.

(3) The peptide CONH group gives rise to two characteristic lines: one near 1660 cm^{-1} (amide I) and the other near 1260 cm^{-1} (amide III). These two frequencies are useful in assessment of conformational changes in proteins.

(4) Lines in the region from 800 to 1150 cm^{-1} due to the skeletal stretching of polypeptide backbone and side chains are expected to be conformational-dependent.

(5) The C-S stretching frequencies due to a methionine residue depend on the conformation of its side group, $-CH_2CH_2SCH_3$. Two lines at 655 and 724 cm^{-1} are expected for the trans form and one line at 700 cm^{-1} together with a shoulder for the gauche form. In the spectrum of ribonuclease, no lines are observed at 700 ± 6 cm^{-1}, suggesting that all four methionine side groups in ribonuclease are in the trans form.

Although they have obtained a great deal of significant new structural information of these proteins in the native states, Raman spectra of denatured proteins were not obtained at that time because of the experimental difficulties associated with the optical inhomogeneity of the sample and the use of a low power, low frequency He-Ne laser. In the present work, the author has employed a high power, high frequency argon-ion laser as an excitation source to obtain Raman spectra of glucagon, insulin, and proinsulin (Figure 1). Glucagon was used as a model compound to study the Raman spectral changes associated with the α-helix-coil-β transition in proteins. Comparisons will be made between the spectra of native and denatured insulin (Figure 2) and those of native insulin in crystals and in solution at various pH's. Structural information derivable from such comparisons will be discussed in detail. In addition,

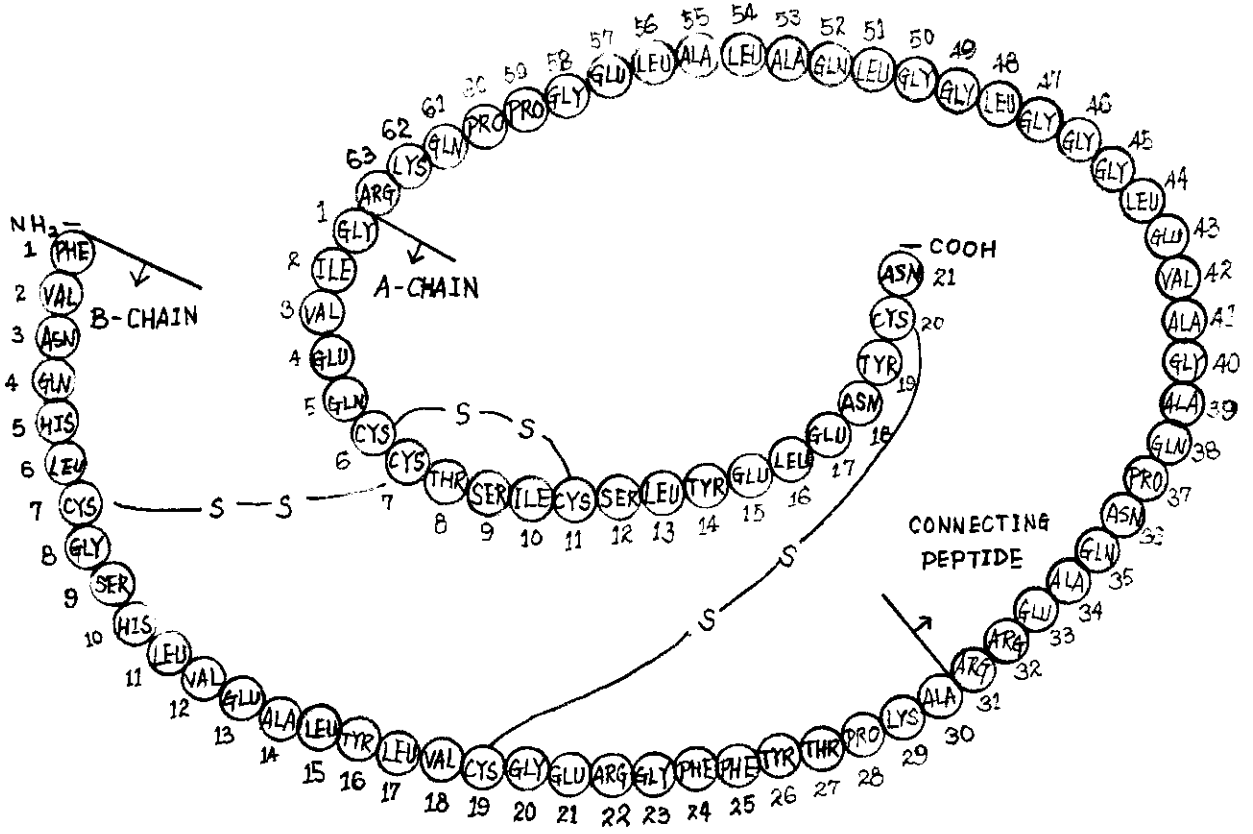

Figure 1. The Primary Structure of Procine Proinsulin

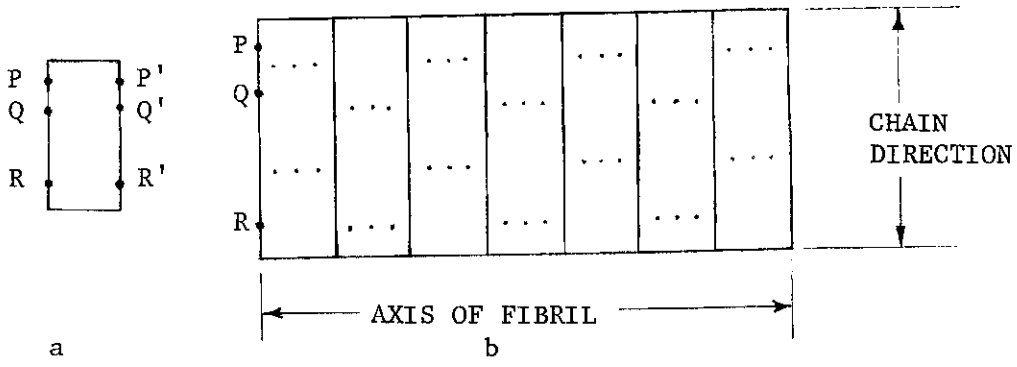

a: Native insulin molecule.

b: The interchain hydrogen bonded grid structure of fibrous insulin (Cross-β conformation).

P, Q, R: Side groups on the opposite side of the molecule.

P', Q', R': Side groups along the side of native molecule and parallel to the primarily folded chains.

Dotted lines: Hydrogen bonds between N-H and C=O groups.

Figure 2. Proposed Mechanism for the Denaturation of Insulin (from Ambrose and Elliott, 1951)

the spectra of insulin and proinsulin in the solid state will also be compared.

CHAPTER II

INSTRUMENTS AND METHODS

Instruments

The laser Raman system consists of four parts:

(1) Source of Excitation:

The Coherent Radiation model 52B argon-ion laser is the source of excitation for Raman spectroscopy. A high-current gas arc-discharge tube, which is excited with direct current and placed in an optical cavity, is its principal component. It also contains a gas supply system and a cooling system which cools the power supply and laser head. The 52B laser emits a minimum of two watts in the blue-green region of the visible spectrum (457.9; 465.8; 472.7; 476.5; 488.0; 496.5; 501.7, and 514.5 nm) with the principal laser emission at 488.0 and 514.5 nm.

The power supply provides dc power to the laser tube and magnet by means of rectification directly from a three-phase, 208 v, power line.

(2) Optical System:

After passing through an interference filter, which removed the plasma emission lines, the laser beam was then focused, by a lens, and reflected by a mirror upward onto the surface of solid sample or upward through the capillary cell of solution sample. The scattered light was collected by a f/1.1 lens and imaged with a 3:1 magnification on the entrance slit of a Spex 1401 double monochromator.

(3) Double Monochromator:

This is the analyzer of scattered light. It consists of two gratings for double dispersing, six reflection mirrors, and three slits.

The scattered light comes through slit 1 and is reflected by mirror 1 to grating 1. The dispersed light is then under successive reflection by mirrors 2, 3, 4, and 5 to grating 2. In this path the light has passed slit 2 between mirrors 3 and 4. Finally, the doubly dispersed light goes through the third slit to the photomultiplier by the reflection of mirror 6.

(4) Detector and Signal Analyzer:

The light is detected by an ITT FW-130 photomultiplier which is thermoelectrically cooled to reduce the dark count rate to a few counts per second by a Products for Research, Inc. model TE-104 thermoelectric refrigerated chamber. This chamber provides cooling for the photomultiplier tube to at least $-20^{\circ}C$.

The photomultiplier signal is amplified and processed by the photon counting system which consists of: Tennelec model Aec-1000 bin and power supply, PAD model ND-520 preamplifier and amplifier, Tennelec model TC-590 ratemeter, and Electronik model 194 recorder.

A different holder for solid and solution samples is needed:

(1) Solution Sample Holder:

A Cary Instruments' kinematic base and backing mirror assembly was used to hold a capillary cell. The cell, which is 1 mm I.D. x 25 mm long with a fire-polished flat end and made of Pyrex contained about 10 microliters of solution and was held vertically. The laser beam

entered the cell from the flat end and went through the solution. The light scattered at 90 degrees to the incident beam and was then collected and focused onto the first slit of the double monochromator.

(2) Solid Sample Holder:

The sample in powder form was packed into the conical cavity at the end of the rod. The sample rod was mounted on a Cary Instruments' kinematic base. The laser beam was focused onto the sample at the grazing angle so that the scattering column was a strip on the powder surface, one-eighth inch long and approximately 40 microns wide. The scattered light was then collected and focused onto the entrance slit (slit 1) of the double monochromator.

The arrangement of the various parts of the laser Raman system is shown in Figure 3.

Instrumental Method

The monochromatic beam at 514.5 nm wavelength from the laser passed through an interference filter which removed the argon emission line and was then reflected upward and focused onto the sample. Scattered light from the solid sample surface or solution was collected by another lens and focused onto the entrance slit of the double monochromator. The output of the monochromator was detected by the photomultiplier tube. The photoelectron pulses from the phototube were counted passed through a photon counting system and displayed on a strip chart recorder.

For solid samples the laser power, as measured with a Coherent Radiation power meter, was usually from 144 to 198 mW. Since the

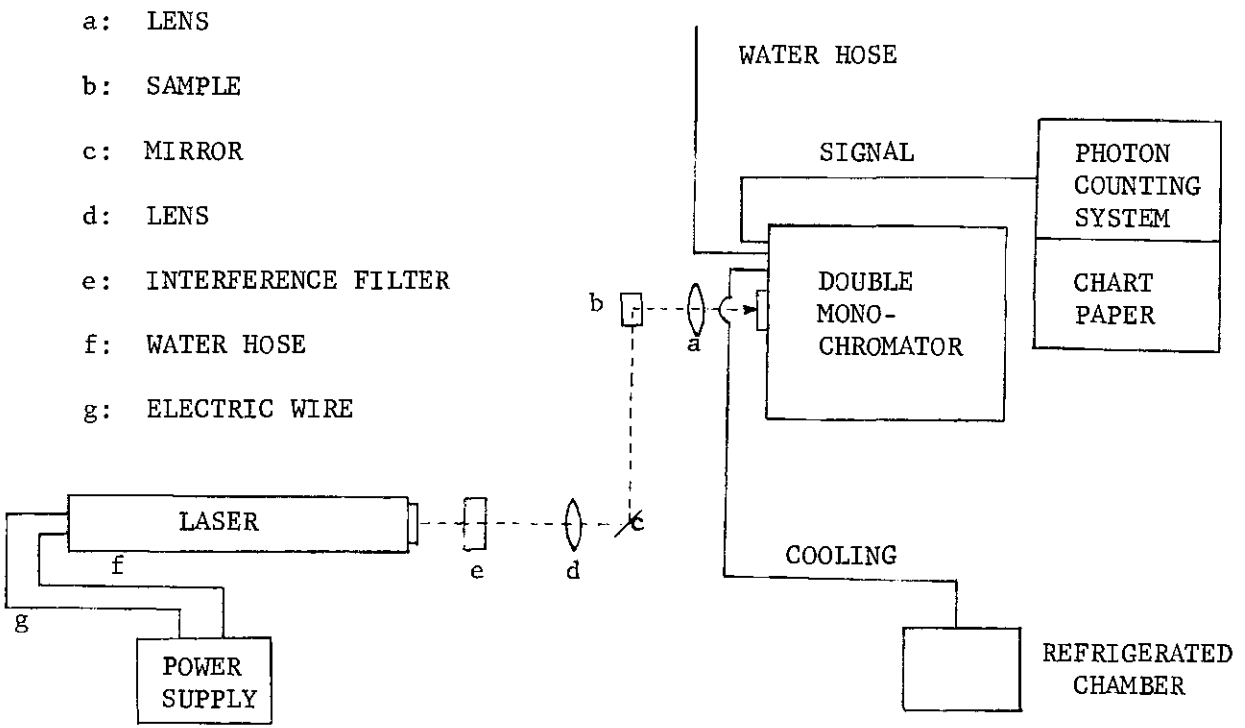

Figure 3. The Arrangement of the Various Parts of the Laser Raman System

intensity of Raman lines is proportional to the power at the sample, the higher the power the better the signal-to-noise ratio. However, too high power could result in burning solid samples. Laser power for solution samples could be somewhat higher and was usually from 450 to 540 mW.

The spectrum is recorded with the intensity of Raman scattering in relative units on the ordinate scale and wave number displacement is cm^{-1} from the laser exciting frequency which is taken as the zero of the abscissa scale.

The spectral slit width for all the spectra reported in this thesis is approximately 4 cm^{-1} and the accuracy of the wave number is $\pm$ 1 cm^{-1}.

CHAPTER III

MATERIALS AND SAMPLE HANDLING

Bovine and porcine insulin (twice crystallized) were obtained from Schwarz/Mann and recrystallized before experiments according to the method of Schlichtkrull (1956). Porcine proinsulin of high purity (98 percent single component material) was a gift from Dr. R. E. Chance of the Lilly Research Laboratories, Indianapolis, Indiana. This sample was a lyophilized powder (from acetic acid) and used without further purification. Crystalline glucagon was also obtained from Schwarz/Mann and used without further purification.

Doubly distilled, degassed water and 0.1 M HCl (or 0.1 M NaOH) were used in preparing the solutions of insulin at various pH's. The pH values were measured by a Radiometer pH meter model 26 with a microprobe combination electrode to the accuracy of ± 0.01 pH unit. Before injection into the capillary cell, solution samples were centrifuged in an International Equipment Refrigerated Centrifuge at a speed of 7,000 rpm for one-half hour in order to eliminate solid particles.

Three samples of denatured insulin were prepared according to the following procedures: (A) a solution of 10 mg/ml insulin at pH 2.42 was heated at 100°C for 45 minutes. The solid sample was obtained by air-drying the resulting fibrous gel. (B) same as for (A) except a tenfold increase in the concentration of solution. (C) a solution of 10 mg/ml

insulin at pH 2.42 was seeded by 0.5 mg per milliliter of denatured insulin obtained from (A) for three days at 25°C. The resulting gel was then subject to air-drying. The denatured insulin prepared in this way was referred to as insulin fibrils in the literature (Waugh, 1944).

CHAPTER IV

RESULTS AND DISCUSSION

Raman Spectra of Glucagon in Various States of Aggregation — A Model System for Proteins

The spectral regions in 1630-1700 cm^{-1} (amide I) and 1220-1300 cm^{-1} (amide III) are useful for studying conformational features of the polypeptide backbone in Raman spectra. The amide I and III vibrational modes in the Raman spectra of polypeptides of known α-helical structure occur at different frequencies from those of β-pleated sheet or random-coil structure. In Table 1, the amide I and III frequencies (in cm^{-1}) of model compounds in various conformations are listed. It seems that the data from model compounds can be used to assign the amide I and III frequencies of proteins and for quantitative measurement of the relative amount of ordered structure in a protein. However, there is some reluctance to accept these as characterizing frequencies for various conformations in proteins. This is because peptide homopolymers have symmetry elements in the α-helix and β-structure. Selection rules can then restrict both the number and position of frequencies that may appear in the spectrum. In the case of proteins, because of the variety of side groups, no symmetry elements exist and there should be no symmetry restriction. Glucagon was then used as a model compound to study the Raman spectral changes associated with the α-helix-to-coil-to-β transition in protein.

Glucagon is a polypeptide hormone of 29 amino acid residues with a known sequence. It has been reported that it exists in 75 percent α-helical structure in crystals and that in freshly prepared acidic solutions, glucagon is predominantly in the form of a random coil. On standing at 26°C, this acidic solution is gradually converted into a gel, which is found to consist of antiparallel-β chains (Gratzer, 1967; 1968).

In Figure 4 are presented the Raman spectra of glucagon in crystals, freshly prepared aqueous solution (pH 2.25) and gels. In descending order, these spectra show a stepwise decrease in frequency of the amide III lines from 1266 (α-helix) to 1248 (random-coil) and then to 1232 cm^{-1} (antiparallel-β). These frequencies are very similar to those of α-helical poly-L-glutamic acid and antiparallel-β polyglycine I, respectively. In the 1630-1700 cm^{-1} region, the amide I line of crystalline glucagon is seen at 1658 cm^{-1}. The shoulder near 1685 cm^{-1} may be due to the unsolvated random-coiled segments of glucagon (about 25 percent). It is of interest to note that, in the amide III region, there also exists a shoulder at 1235 cm^{-1}, which may be associated with the same structure (random-coil). In Figure(b) the strong water line near 1640 cm^{-1} has obscured the amide I frequency of glucagon in freshly prepared aqueous solution. Upon gel formation, however, the amide I line has sharpened considerably and showed up in the spectrum (Figure 4(c)) as an intense sharp line at 1672 cm^{-1} (half-width about 15 cm^{-1}) on the sloping background of water. Again, the two frequencies, 1658 and 1672 cm^{-1}, are in agreement with the corresponding amide I frequencies of α-helical poly-L-alanine and poly-glycine I. On the basis of present results, it appears that the

substitution of homo-side-chains in synthetic polypeptides by a variety of side groups does not affect the frequencies of the strongly coupled amide I and III vibrations as much as might be expected.

In order to compare the results from two different methods, the infrared data are also listed in Table 1. It is evident that there is little agreement. This is not due solely to experimental error. Rather, the discrepancies are due to excitation of coupled vibrations between adjacent peptide units. In the case of model compounds, symmetry can restrict modes to be Raman-active, infrared-active or inactive, and the differences in frequencies reflect different normal vibrations of a coupled system. In the case of proteins, however, no such symmetry exists and all vibration should be Raman and IR active. However, these vibrations retain a large oscillating dipole moment or large differential polarizability making them "infrared-intense" or "Raman-intense" vibrations.

Raman Spectra of Denatured Insulin

Comparison of Raman Spectra of Native and Denatured Insulin in the Solid State

Insulin is a protein hormone whose three dimensional structure has recently been determined with x-ray analysis at a resolution of 2.8 Å by Hodgkin and his associates (Adams et al., 1969).

Denatured fibrous insulin is formed at pH ~ 2 by heating at a temperature greater than 80°C, with a concomitant loss in biological activity and solubility. However, both the activity and solubility can be recovered by treatment with alkali at 0°C and pH 11.5.

Raman spectra of native and denatured insulin in the solid state are shown in Figure 5. After removing the noise, they are redrawn and superimposed for comparison in Figure 6. The measured vibrational frequencies in cm^{-1} are listed in Table 2.

Under the comparison, it was found that numerous spectral changes have taken place upon denaturation. From the reversibility of the biological activity, as mentioned above, of insulin (Waugh, 1954), it is assumed that all these changes are the reflections of the changes in molecular conformation.

First, the amide I line has shifted from 1662 cm^{-1} with a shoulder near 1685 cm^{-1} to 1673 cm^{-1} and sharpened considerably upon denaturation. A similar spectral change has been observed not only in the process of gel formation of glucagon but also in work on the chemical denaturation of lysozyme by Lord (1971) and Mendelsohn (1972). They found that the amide I has shifted from 1660 cm^{-1} in native lysozyme to 1675 cm^{-1} in S-cyanoethylated lysozyme and sharpened also. These were interpreted by these authors as due to the weakening of hydrogen bonding and the sharpening of the amide I line as a reflection of the greater uniformity in the H-bonding. Changes in strength of hydrogen bonds in the amide groups will affect the frequency of the C=O stretching (amide I) vibration and a stronger H-bond gives rise to a lower stretching frequency (amide I) (Richards and Thompson, 1947). This interpretation, however, is incomplete. Coupling between the adjacent peptide groups may have an effect on these. Both the infrared results of Ambrose and Elliott (1951) and the present Raman study have shown the evidence of strong

coupling between adjacent peptide groups. In the infrared studies of denatured insulin, Ambrose and Elliott found the infrared amide I shifted from 1657 to 1637 cm^{-1} upon denaturation. To confirm their result, the infrared spectra of native and denatured insulin (in Nujol) in the amide I region were reobtained and the comparison between the infrared and Raman results is shown in Figure 7. In the denatured state, one coupled mode gives rise to the Raman-intense line at 1673 cm^{-1}, while the other coupled mode appears as an infrared-intense band at 1635 cm^{-1}.

Because of its reversibility, the conformation of denatured fibrous insulin had been suggested as the linear aggregate of only slightly distorted native insulin (Waugh, 1944; Koltun et al., 1954; Reithel, 1963; Beaven et al., 1969). However, on the basis of infrared dichroism studies on synthetic polypeptides and denatured insulin, Ambrose and Elliott (1951) concluded that denatured insulin consists of extended chains lying **perpendicular** to the fibril axis, with a layer structure involving interchain hydrogen bonded grids (i.e., cross-β-structure). Thus, a mechanism of insulin denaturation was proposed as a change from intrachain to interchain hydrogen bonds when insulin was denatured (Fig. 2). Recently, Burke and Rougvie (1972) have conducted electron microscopy, low angle x-ray diffraction, UV circular dichroism, and IR dichroism studies and affirmed the essential correctness of the Ambrose and Elliott proposal. The Raman spectroscopic conclusion about the β-structure of denatured insulin can be readily drawn from the comparison between the amide I and III frequencies of denatured insulin and those of model compounds. From these data, however, one cannot tell whether this is parallel or antiparallel form.

The next spectral change occurs in the amide III region. In this region, the "center of gravity" of the complex line shape has shifted from 1260 cm^{-1} to about 1230 cm^{-1}. In the work on denaturation of lysozyme, Lord (1971) and Mendelsohn (1972) also observed that the amide III line had shifted from 1260 to 1247 cm^{-1} upon denaturation. For the denatured insulin, the spectral feature at 1230 cm^{-1} agrees with the amide III frequency of the model compounds with known β-structure and with the conclusion drawn from the amide I line.

The region from 450 to 700 cm^{-1} contains the information of the S-S and C-S stretching vibrations of the C-S-S-C group. From the vibrational frequencies and the intensities, the dihedral angle and C-S-S bond angle can be determined. When insulin is denatured, the spectral changes in this region are quite obvious. The peak intensity of the S-S frequency has increased, and the line at 668 cm^{-1} has shifted to 657 cm^{-1} with a considerable decrease in intensity. The line at 678 cm^{-1} slightly shifted to 680 cm^{-1} with no appreciable change in intensity. This observation suggests that the geometry of the two interchain disulfide links in the denatured state is different from that in native form and that the intrachain one remains in nearly the same conformation upon denaturation.

The skeletal bending frequencies occur in the region below 800 cm^{-1} and are very sensitive to protein conformation. In Table 2, seven Raman lines in the spectrum of native insulin are tentatively assigned to this category. Numerous spectral changes between 470 and 800 cm^{-1} are clearly shown in Figure 6. Upon denaturation, the lines at 495 and 563 cm^{-1} disappear and a new line at 532 cm^{-1} appears and, in the region near 750 cm^{-1},

instead of resolving into three lines at 725, 747, and 777 cm^{-1} as in native form, these three lines coalesce into one peak at 737 cm^{-1}. Based on normal mode vibration calculations of model compound N-methyl-acetamide, Miyazwa et al. (1958) have assigned a line near 725 cm^{-1} to the N-H out-of-plane bending (i.e., amide V). Since deuteration of denatured insulin does not result in a complete disappearance of the 737 cm^{-1} feature from the spectra, the assignment of the triplet near 750 cm^{-1} to specific conformational components of native form and that of the single line at 737 cm^{-1} to the β-conformation is tentative.

As Lord and Yu (1970a) predicted earlier, the C-C and C-N coupled skeletal stretching in the 800 to 1220 cm^{-1} region should show spectral changes on denaturation. The drastic changes of lines at 900, 935, 946, 963, and 1112 cm^{-1} indicate that an extensive unfolding of the protein backbone has occurred. Since the native insulin crystals were grown at neutral pH and the denatured insulin was prepared at pH 2.42, one might wonder if the spectral changes are caused partially by the presence of HCl in the denatured sample. A Raman spectrum of native insulin HCl solid is shown in Figure 9A. The protonation of the carboxyl groups and imidazole rings does produce slight changes in this region. However, the spectra of native insulin HCl solid and denatured insulin are still drastically different in this region. The line at 1128 cm^{-1} cannot be attributed to one of the characteristic ring frequencies of the aromatic side groups and is found to be independent of conformation. This line was also observed in the spectra of α-chymotrypsin (Lord and Yu, 1970b). In general, spectral lines in this region are not well understood.

Raman Spectra of Denatured Insulin Obtained under Different Conditions

The denatured insulin whose spectrum was compared with that of native insulin in the previous section was prepared by heating at 100°C for 45 minutes and air-drying the resulting sample. In Figure 8A is the spectrum of denatured insulin which was prepared under the same conditions except for a tenfold increase in concentration. The spectrum of denatured insulin solid obtained by seeding (Waugh, 1954) is shown in Figure 8B. Identical x-ray diffraction patterns of both denatured insulins obtained by heating and seeding have been observed by Koltun et al. (1954). A few noteworthy differences, however, can be detected through the comparison between Figure 5B and Figure 8A and B. The C-S stretching line near 668 cm^{-1} is much weaker in both spectra in Figure 8. A change in the C-S-S bond angle is then related as it was pointed out by Lord and Yu (1970a). To the extent that the analogy with the spectra of crystalline cystine and dimethyl disulfide can be made quantitative, it appears that the C-S-S angles of the three disulfide links in these latter examples of denatured insulin are about 114° and those in the native insulin about 103°. Also, small changes in the amide V region around 750 cm^{-1} and the new line at 1020 cm^{-1} in Figure 5B may appear as either the shoulder of the 1032 cm^{-1} line or that of the 1004 cm^{-1} line in Figure 8A and B, depending on the conditions of denaturation. The amide III line appears to be resolved at 1227 cm^{-1} in the denatured sample of higher concentration. Except for these minor differences, three spectra of denatured insulin are silimar and the similarity in the amide I and III regions suggests that all denatured insulin exist in the same conformation.

Raman Spectra of Native Insulin in Solution at Various pH's

The spectra of aqueous insulin at pH 2.40 and 8.30 are shown in Figures 9B and 10. No significant changes were observed in the amide I and III regions when the pH value is changed from 2.40 to 8.30. This indicates that no significant conformational changes take place. The spectral changes in the 900-1000 cm^{-1} region might be due to the ionization of the carboxyl groups and imidazonium rings of side chains, whereas the intensity increase at 950 cm^{-1} in the spectrum of aqueous insulin HCl is due to the imidazonium rings of the histidine residues (Yu, 1969).

Small differences can be found when one examines spectra of solid insulin HCl and aqueous insulin HCl (Figure 9A and B). In addition to the slight change in line shape occurring near 950 cm^{-1}, a slight shift in the line shape in the amide III indicates that, on dissolution, the relaxation of the backbone chains and side groups results in a slight increase in random-coil structure.

Raman Spectra of Insulin and Proinsulin in the Solid State

Proinsulin is the precursor of insulin. Its Raman spectrum has been taken and redrawn to remove the noise. Figure 11 shows the comparison between the Raman spectra of insulin and those of proinsulin. It is apparent that more than 11 conformation-dependent lines agree in both spectra. This indicates that the insulin moiety of proinsulin exists in a conformation very nearly the same as insulin itself and that the differences between the two spectra may be the contribution from the connect-

ing peptide (C-peptide). Because the C-peptide does not contain any Phe residues and the 624 cm^{-1} line is considered to be conformation-independent (Lord and Yu, 1970a), the spectra have been normalized by recording them with the 624 cm^{-1} line intensity adjusted to the same value. A graphical subtraction in the amide I region shows that the C-peptide contributes an amide I line at 1663 cm^{-1} with a shoulder near 1685 cm^{-1}. Since these two frequencies are characteristic of α-helical structure and random-coil form, respectively, we conclude that the C-peptide moiety in proinsulin contains a considerable fraction of α-helical structure. In fact, x-ray crystallographic studies (Fullerton, Potter, and Low, 1970) indicated the presence of two short segments of α-helixes in the C-peptide of proinsulin. Frank and Veros (1968) have studied circular dichroism spectra of proinsulin and insulin. They concluded that the insulin moiety existed in the same conformation as in insulin itself and that the connecting peptide took on a random-coil conformation.

Detailed assignment of the vibrational frequencies in cm^{-1} of the Raman spectrum of proinsulin are listed in Table 3.

Table 1. Amide I and III Frequencies (in cm^{-1}) of Model Compounds in Various Conformations

Conformation	Compound	Amide I		Amide III	
		Raman	Infrared	Raman	Infrared
α-helix	poly-L-alanine fibers[a]	1660S	1657S	1264S	1262S
	glucagon (crystalline)[b]	1660S		1266S	
β-structure:					
antiparallel	polyglycine I[c]	1674S	1685M 1636S	1234S	1236M 1214W
				1220W	
	poly-L-lysine[d]	1672S			
	glucagon (gels)[b]	1672S	1630	1232M	
parallel	calculated[e]		1650 1630		
random-coil:					
solvated	poly-L-glutamic acid[f] at pH 10	1665B		1248B	
	glucagon (freshly prepared acidic solution)			1248B	
unsolvated	glucagon[b]	1685		1235	

Note: S, strong; B, broad; M, medium, and W, weak.

[a] Fanconi et al. (1969)

[b] Present work

[c] Small et al. (1970)

[d] Wallach et al. (1970)

[e] Miyazawa (1967)

[f] Lord and Yu (1970b)

Legend for Tables 2 and 3

Vibrational frequencies are expressed as the displacement in cm^{-1} of the Raman lines. The symbol B denotes broad; S, sharp; D, doublet; T, triplet; sh, shoulder; ν(X-Y), a frequency assigned to an X-Y bond-stretching vibration. Figures in parentheses are relative peak intensities based on a value of 10.0 for the strongest line in each spectrum.

Table 2. Raman Spectra of Insulin (bovine) (200-1800 cm^{-1})

Frequencies in cm^{-1} Native (crystals)	Denatured (solid)	Tentative Assignments
	265 (0.9)	skeletal bending
333 (0.9)	325 (0.8)	
410 (0.8)	420 (0.5)	
467 (0.8)	460 (0.4)	
495 (1.2)	480 (0.3)	
515 (3.2)	513 (4.4)	ν(S-S)
	532 (1.5sh)	skeletal bending
563 (1.0)		
624 (2.0S)	624 (2.0S)	Phe
644 (3.6S)	644 (3.6S)	Tyr
668 (2.0)	657 (1.1)	ν(C-S) of the C-S-S-C group
678 (1.0sh)	680 (1.3)	
725 (0.8T)		skeletal bending
747 (0.8T)	737 (0.9B)	
770 (0.8T)		
814 (1.4sh)		
832 (4.4D)	830 (3.9D)	Tyr
854 (5.5D)	853 (4.5D)	
900 (2.0)	882 (1.5)	ν(C-C)
934 (2.0sh)	922 (0.8)	
946 (3.2D)		
963 (2.9D)	956 (1.6B)	
1004 (10.0S)	1004 (10.0S)	Phe
	1020 (2.5)	ν(C-N)
1032 (3.3S)	1032 (3.3S)	Phe
	1057 (1.3sh)	
1112 (1.5sh)		ν(C-N)
1128 (1.8)	1127 (1.7)	
1162 (0.9)	1161 (0.5sh)	
1177 (2.4)	1175 (2.4)	Tyr
1212 (4.6S)	1214 (4.9)	Tyr
	1227 (4.3)	amide III (β-structure)
	1252 (4.0sh)	
1239 (5.0sh)		amide III (random-coil)
1270 (5.3)		amide III (α-helical)
1288 (4.7sh)		amide III (α-helical)

Table 2. (Concluded)

Frequencies in cm^{-1}		Tentative Assignments
Native (crystals)	Denatured (solid)	
1322 (2.0sh)	1327 (2.0D)	CH deformation
1344 (4.0)	1343 (3.1D)	
1367 (1.6sh)		
	1407 (0.4sh)	
1425 (2.5sh)	1422 (1.1sh)	sym. CO_2^- str.
1450 (5.0)	1450 (3.8)	CH_2 deformation
1462 (4.6sh)	1462 (3.1sh)	
1587 (1.3)	1587 (1.0sh)	Tyr
1607 (3.6D)	1607 (3.5D)	Phe
1615 (3.6D)	1615 (3.5D)	Tyr
1662 (4.6)		amide I (α-helical structure)
	1673 (8.6S)	amide I (β-structure)
1685 (4.0sh)		amide I (random-coil)
	1735 (0.4B)	-COOH

Table 3. Raman Spectrum of Porcine Proinsulin (lyophilized powder) (200-1800 cm^{-1})

Frequencies in cm^{-1}	Assignments	Frequencies in cm^{-1}	Assignments
267 (3.8S)	impurity (?)	1004 (10.0S)	Phe
308 (1.0)	skeletal bending	1019 (1.0S)	ν(C-N) of C-peptide
406 (1.0B)		1032 (4.0S)	Phe
445 (0.7)		1081 (0.6)*	ν(C-N)
495 (1.4)*		1106 (1.3)*	
515 (3.2B)*	ν(S-S)	1128 (2.6)	
560 (0.8)*	skeletal bending	1160 (1.5)	
612 (0.3sh)		1177 (3.0)	Tyr
624 (2.1S)	Phe	1206 (5.0S)	Tyr
644 (3.7S)	Tyr	1246 (5.5)	amide III
666 (1.6)*	ν(C-S)	1270 (5.6)	amide III
680 (0.5sh)*		1298 (3.2S)	CH deformation
726 (0.7sh)*	skeletal bending	1314 (1.0sh)	
741 (1.7S)		1341 (6.5)	
750 (0.7sh)*		1420 (1.5sh)	symmetrical CO_2^- str.
769 (0.7)*		1450 (9.5)	CH_2 deformation
814 (2.0sh)	Tyr	1536 (0.4)	
831 (4.4D)		1587 (1.3)	Tyr
853 (5.5D)		1607 (3.6D)	Phe
898 (8.0S)	ν(C-C)	1615 (3.6D)	Tyr
919 (2.5)		1663 (9.0)	amide I
945 (3.6)*		1680 (6.0)	amide I
961 (2.6)*			

Figure Legends for Figures 4-11

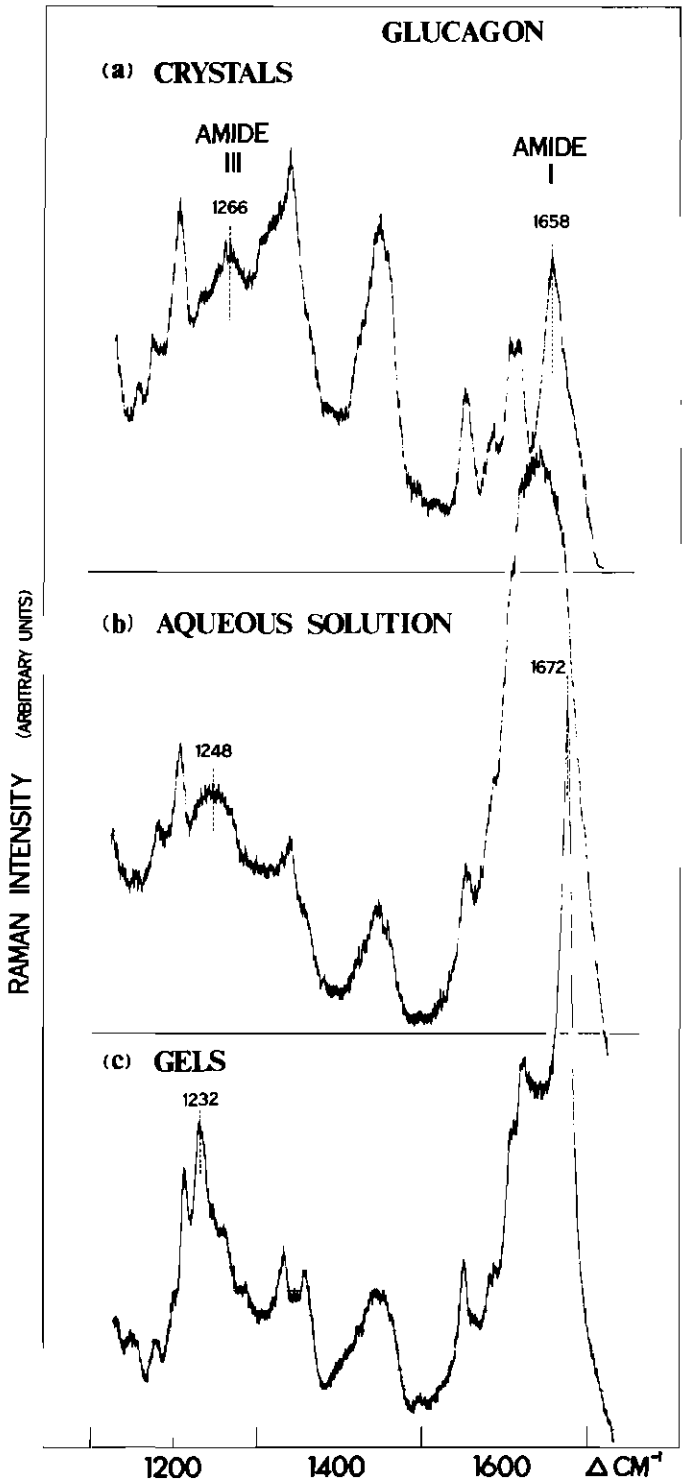

Figure 4. Raman Spectra of Glucagon in Various States of Aggregation

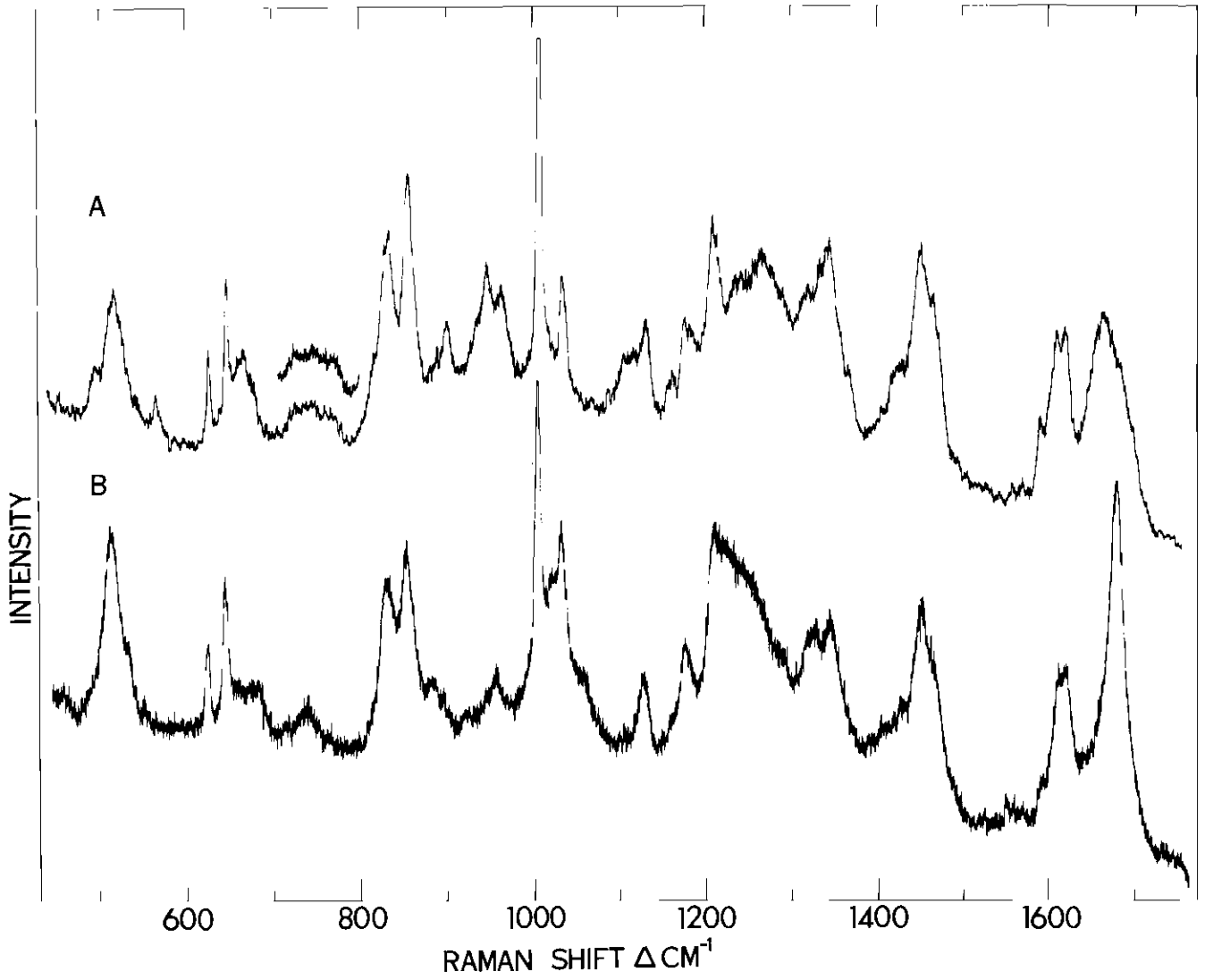

Figure 5. Raman Spectra of Native and Denatured Insulin (bovine) in the Solid State

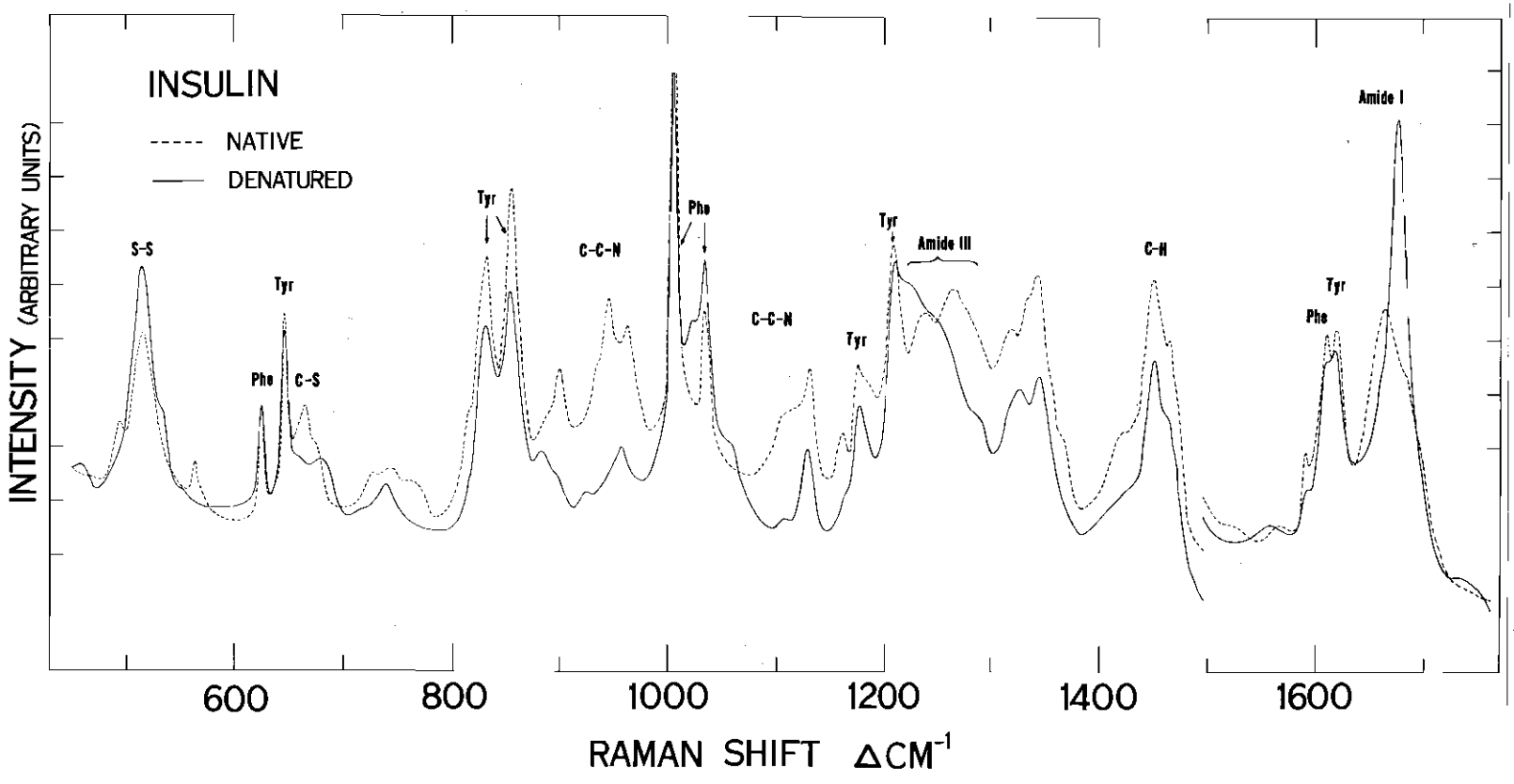

Figure 6. Superimposed Comparison Between the Spectra of Native and Denatured Insulin (redrawn from Fig. 5)

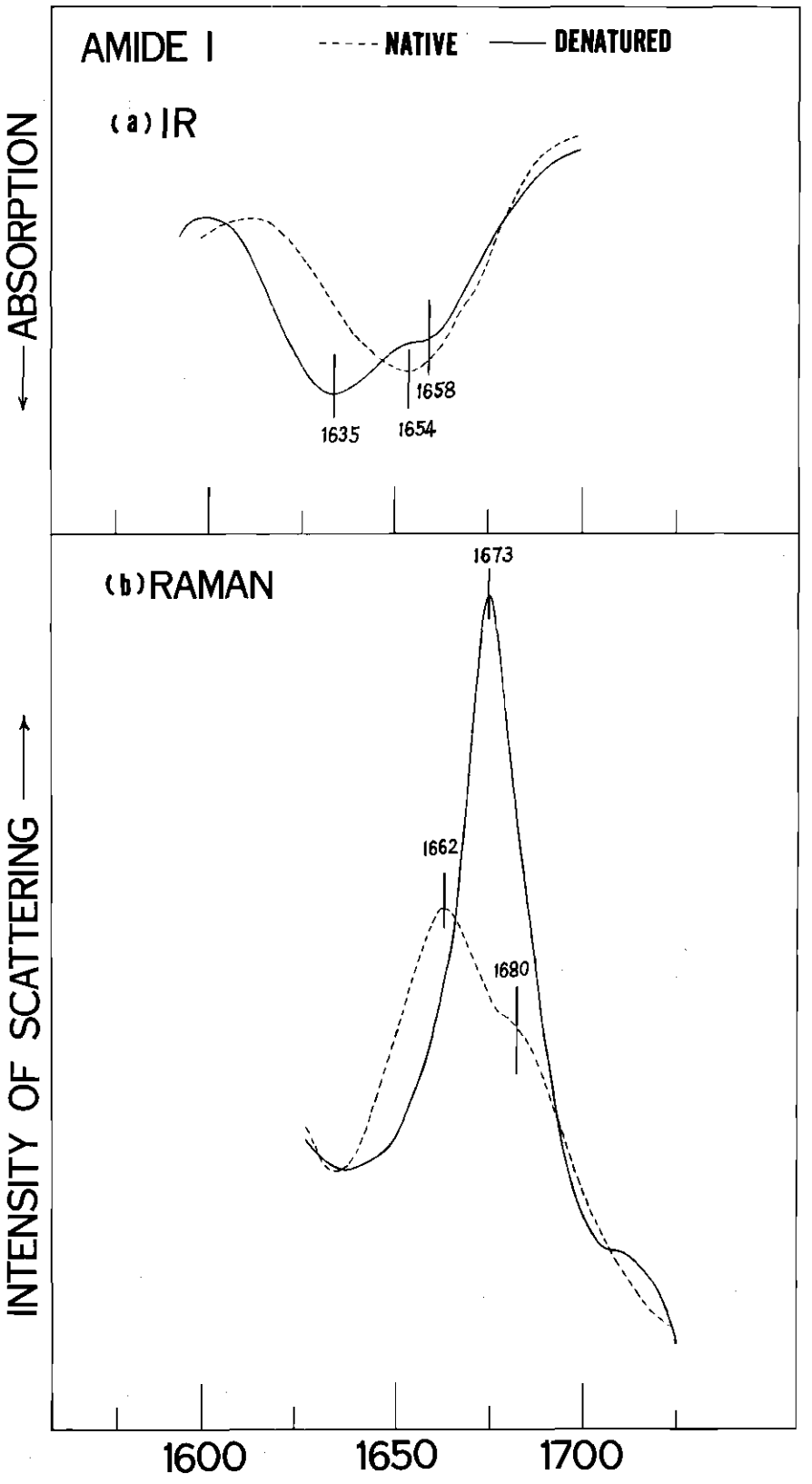

Figure 7. Comparison of Infrared and Raman Amide I Frequencies of Insulin

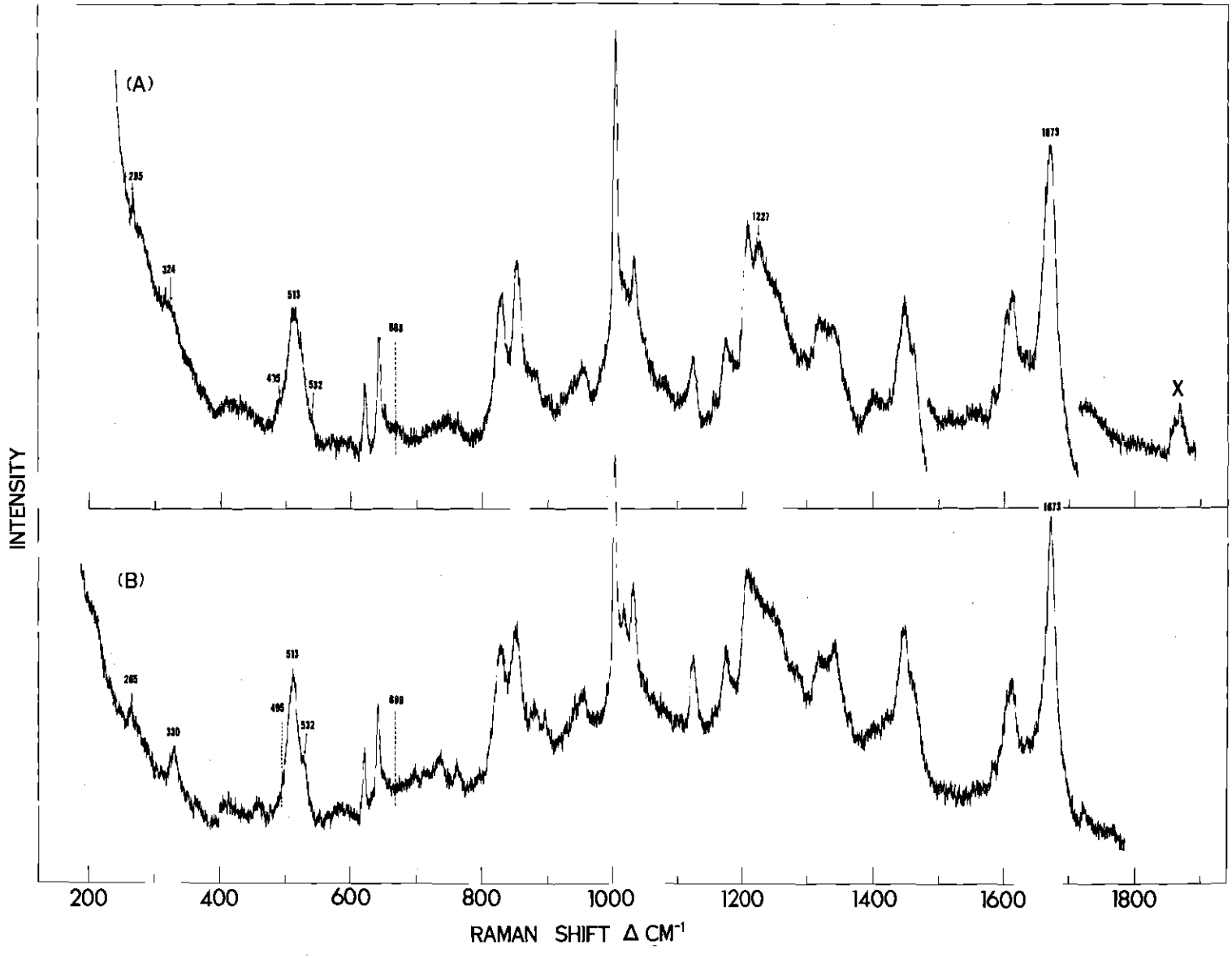

Figure 8. Raman Spectra of Various Denatured Insulin in the Solid State

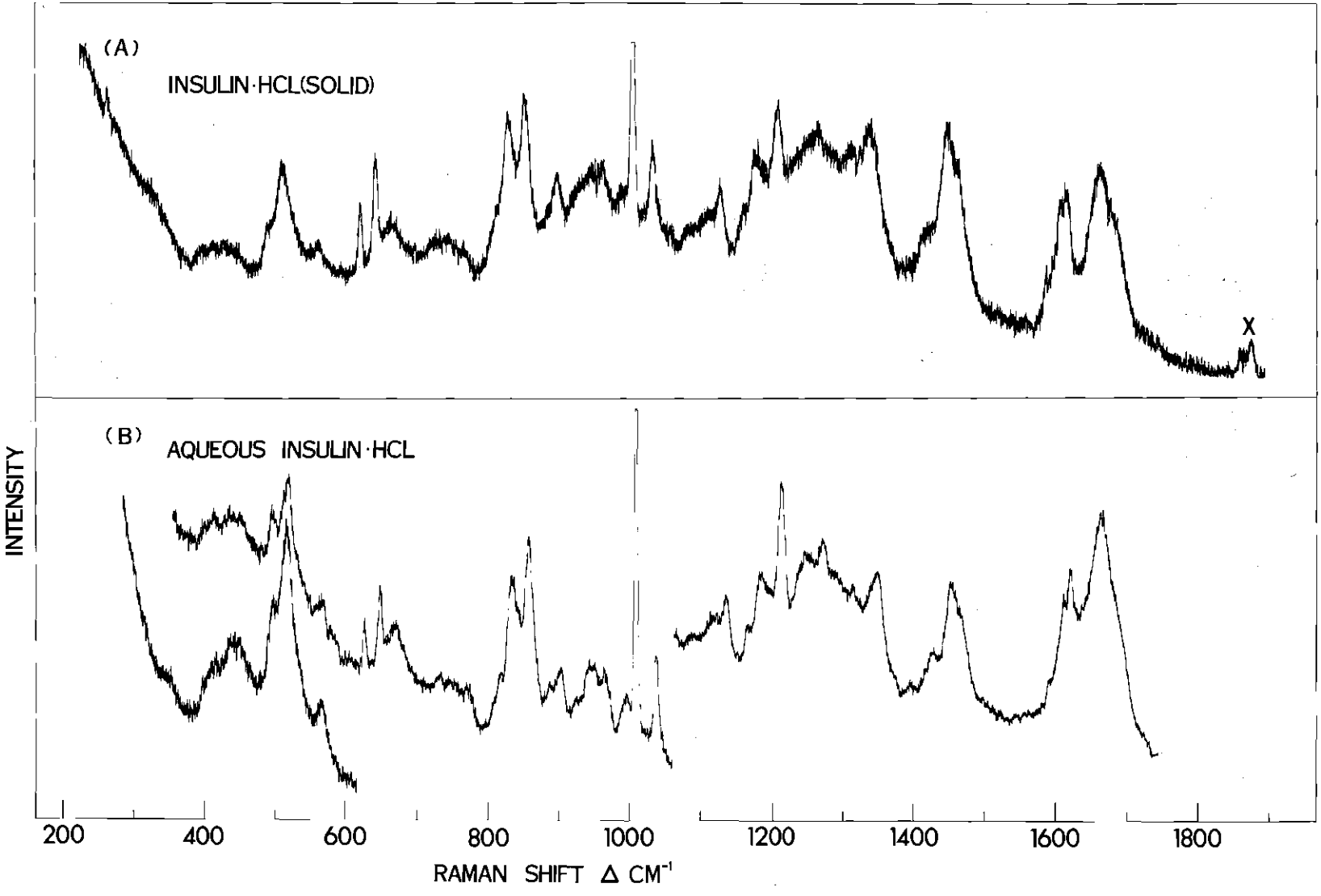

Figure 9. Comparison Between the Raman Spectra of Insulin in the Solid State and in Solution

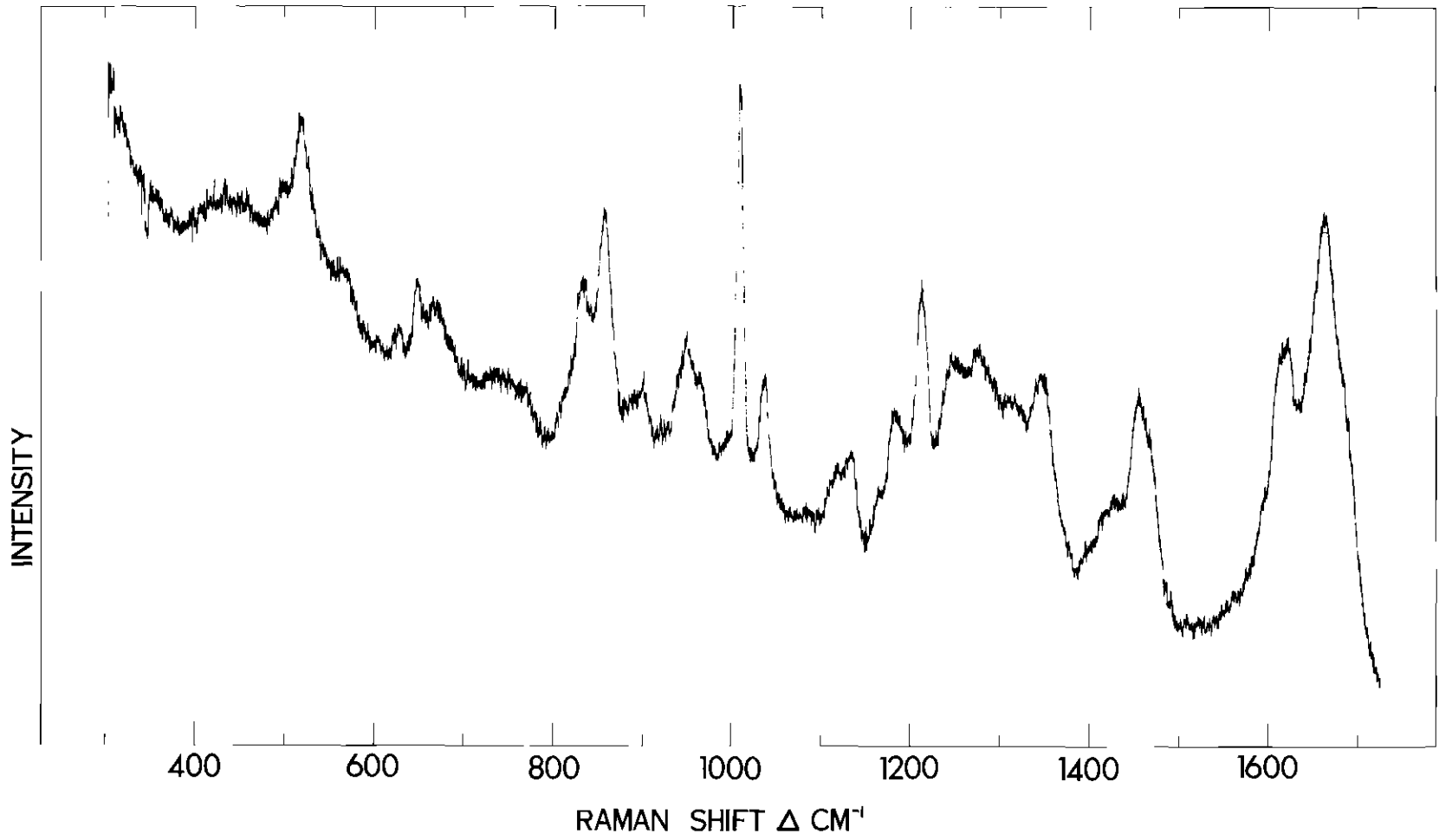

Figure 10. Raman Spectra of Aqueous Insulin at pH 8.50

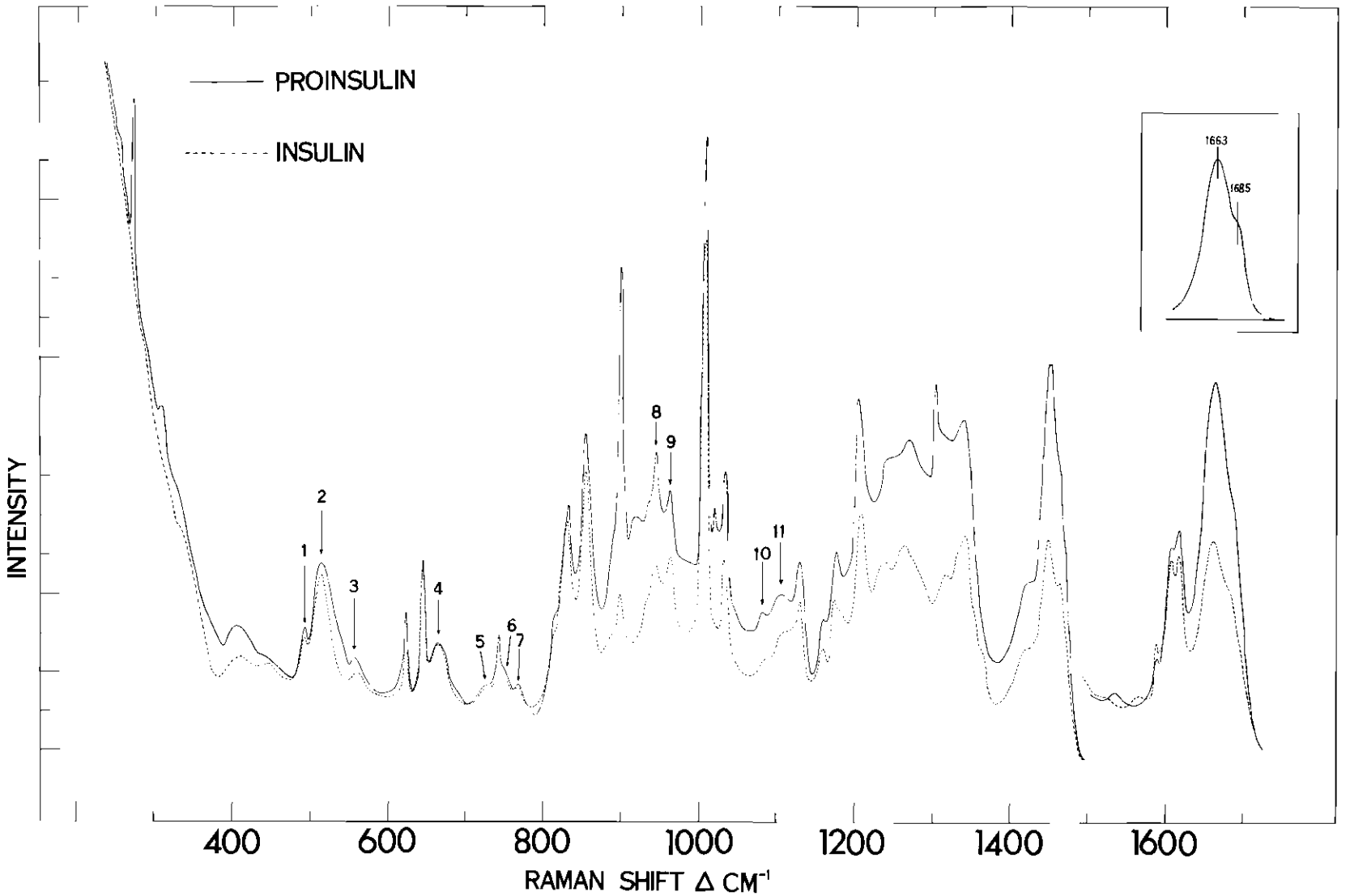

Figure 11. Comparison Between Raman Spectra of Proinsulin and Insulin in the Solid State

CHAPTER V

CONCLUSION

1. Raman spectroscopic characterization of proteins in various conformational states (i.e., α-helical, random-coil, and β-structure) has been established. The amide I and III frequencies of glucagon in various conformations agree with those of homopolypeptides in the corresponding states.

2. On the basis of present studies on the denaturation of insulin, it is concluded that Raman spectroscopy is sensitive to protein conformation.

3. Spectral changes in the skeletal stretching and bending vibration regions are not completely understood. Further investigation on model systems is needed to clarify some points.

4. Structural information about the local geometry of the C-S-S-C links in proteins is valuable since no such data are readily available by other techniques.

5. The most significant part of this work is the establishment of the β-structure of denatured fibrous insulin (or insulin fibrils). This is because in the past the conformation of insulin fibril had been considered as the linear aggregate of slightly distorted globular insulin.

BIBLIOGRAPHY*

Adams, M. J., Blundell, T. L., Dodson, E. J., Dodson, G. G., Vijayan, M., Baker, E. N., Harding, M. M., Hodgkin, D. C., Rimmer, B., and Sheat, S., Nature 224, 491 (1969).

Ambrose, E. J. and Elliott, A., Proc. Roy. Soc. (London) Ser. S. 208, 75 (1951).

Beaven, G. H., Gratzer, W. B., and Davies, H. G., Eur. J. Biochem. 11, 37 (1969).

Bellocq, A. M., Lord, R. C., and Mendelsohn, R., Biochim. Biophys. Acta, in press (1972).

Blundell, T. L., Cutfield, J. F., Cutfield, S. M., Dodson, E. J., Dodson, G. G., Hodgkin, D. C., Mercola, D. A., and Vijayan, M., Nature 231, 506 (1971).

Bromer, W. W., Sinn, L. G., and Behrens, O. K., J. Am. Chem. Soc. 79, 2807 (1957).

Burke, M. J. and Rougvie, M. A., unpublished results (1972).

Dixon, G. H. and Wardlaw, A. C., Nature 188, 721 (1960).

Du, Y. C., Zhang, Y. S., Lu, Z. X., and Tsou, C. L., Sci. Sinica 10, 84 (1961).

Edsall, J. T., Cold Spring Harbour Symp. Quant. Biol. 6, 40 (1938).

Fanconi, B., Tomlinson, B., Nafie, L. A., Small, W., and Peticolas, W. L., J. Chem. Phys. 51, 3993 (1969).

Fullerton, W. W., Potter, R., and Low, B. W., Proc. Natl. Acad. Sci. U. S. 66, 1213 (1970).

Frank, B. H. and Veros, A. T., Biochem. Biophys. Res. Comm. 32, 155 (1968).

Garfinkel, D. and Edsall, J. T., J. Am. Chem. Soc. 80, 3818 (1958).

*Abbreviations used herein conform to those found in Chemical Abstracts, 1972.

BIBLIOGRAPHY (Continued)

Gratzer, W. B., Beaven, G. H., Rattle, H. W. E., and Bradburg, E. M., Eur. J. Biochem. 3, 276 (1968).

Gratzer, W. B., Bailey, E., and Beaven, G. H., Biochem. Biophys. Res. Comm. 28, 914 (1967).

Haugen, W. P. and Lipscomb, W. N., Acta Cryst. A-25 (suppl.), S185 (XV-25) (1969).

Hendra, P. J. and Gilson, T. R., Laser Raman Spectroscopy, Wiley-Interscience, New York and London, 1970.

King, M. V., J. Mol. Biol. 11, 549 (1965).

Koenig, J. L., Appl. Spectry. Revs. 4, 233 (1971).

Koenig, J. L., J. Poly. Sci. Part D (1972).

Koenig, J. L. and Sutton, P. L., Biopolymers 8, 167 (1969); 9, 1229 (1970).

Koltun, W. L., Waugh, D. F., and Bear, R. S., J. Am. Chem. Soc. 76, 413 (1954).

Lord, R. C., XXIIIrd Intl. Cong. Pure Appl. Chem., Supplement to Pure and Appl. Chem. 7, 179 (1971).

Lord, R. C. and Mendelsohn, R., J. Am. Chem. Soc. 94, 2133 (1972).

Lord, R. C. and Thomas, G. J., Dev. Appl. Spectroscopy 6, 179 (1968).

Lord, R. C. and Yu, N. T., J. Mol. Biol. 50, 509 (1970a); 51, 203 (1970b).

Low, B. W. and Shoemaker, C. B., Acta Cryst. 12, 893 (1959).

Mendelsohn, R., Ph.D. Dissertation, Massachusetts Institute of Technology (1972).

Miyazawa, T., in Poly-α-Amino Acids (edited by Fasman, G. D.), p. 69, Marcel Dekker, Inc., New York, 1967.

Richards, R. E. and Thompson, H. W., J. Chem. Soc., p. 1248 (1947).

Reithel, F. J., Adv. in Protein Chem. 18, 159 (1963).

Schiffer, M. and Edmundson, A. B., Biophys. J. 10, 293 (1970).

BIBLIOGRAPHY (Concluded)

Schlichtkrull, J., Acta Chem. Scand. 10, 1455 (1956a); 10, 1459 (1956b).

Small, E. W. and Peticolas, W., Biopolymers 10, 69 (1971).

Small, E. W., Fancoli, B., and Peticolas, W. L., J. Chem. Phys. 52, 4369 (1970).

Smith, M., Walton, A. G., and Koenig, J. L., Biopolymers 8, 29 and 173 (1969).

Steiner, D. F. and Clark, J. L., Proc. Natl. Acad. Sci. U. S. 60, 622 (1968).

Sutton, P. and Koenig, J. L., Biopolymers 9, 615 (1970).

Thomas, G. J., Mediros, G. C., and Hartman, K. A., Biochem. Biophys. Res. Comm., in press.

Thomas, G. J., Biochim. Biophys. Acta, 213, 417 (1970).

Timasheff, S. E., Susi, H., and Stevens, L., J. Biol. Chem. 242, 5467 (1967).

Tobin, M. C., Laser Raman Spectroscopy, Wiley-Interscience, New York, 1970.

Waugh, D. F., J. Am. Chem. Soc. 66, 663 (1944).

Waugh, D. F., Adv. in Protein Chem. 9, 326, see reference cited therein (1954).

Wallach, D. R. H., Graham, J. M., and Oseroff, A. R., FEBS letters 7, 330 (1970).

Yu, Nai-Teng, Ph.D. Dissertation, Massachusetts Institute of Technology (1969).